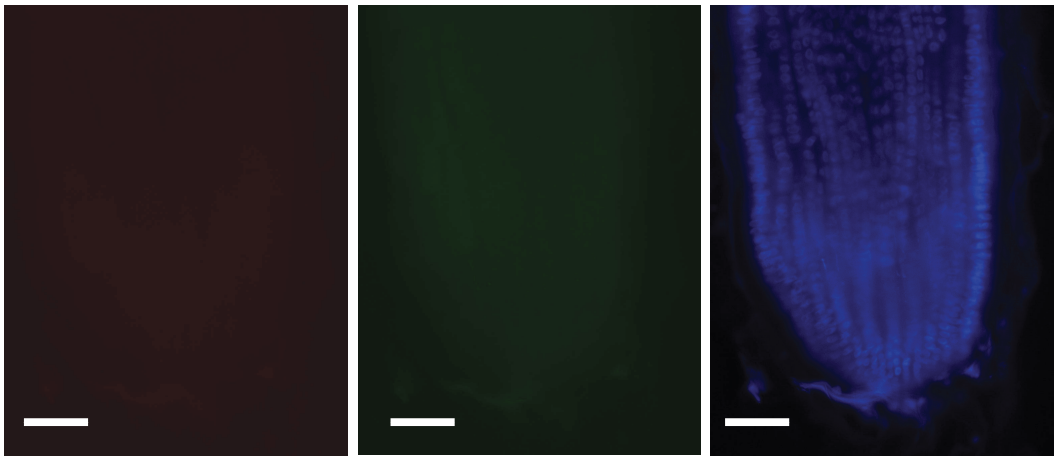

Supplemental Figure 1. Wild-type oat root sections probed with pre-immune sera corresponding to the immuno-localisation images shown in Figure 4 D. Scale bars indicate 100 μm.

Supplemental Figure 2

A

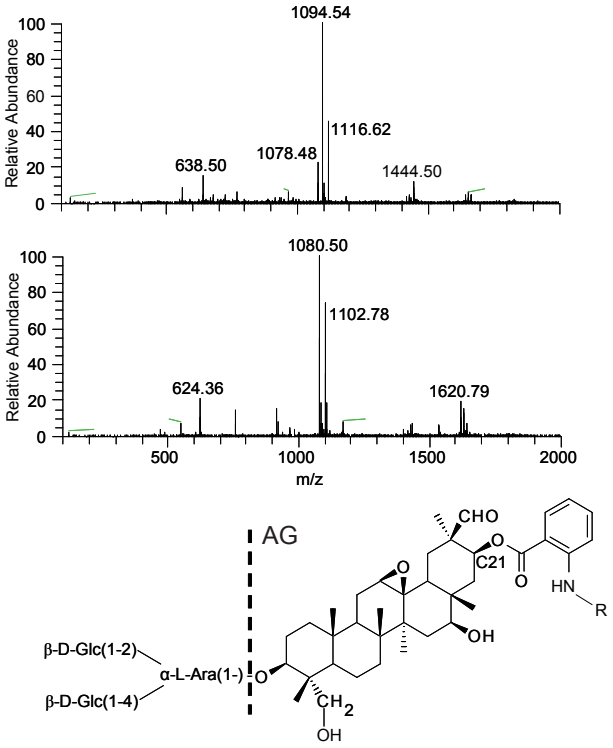

	R	[M+H]	[M+Na]	AG[M+H]
Avenacin A-1	CH3	1094	1116	638
De-methyl avenacin A-1	H	1080	1102	624

B

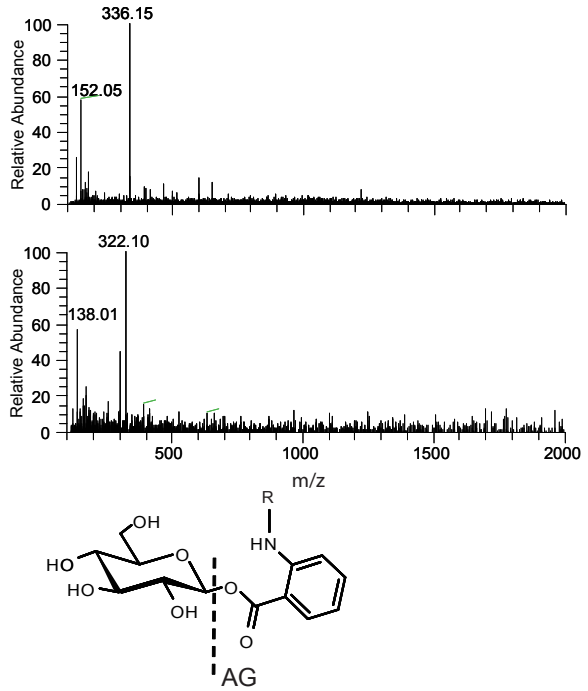

	R	[M+Na]	AG[M+H]
N-methyl anthraniloyl -O-glucose	CH3	336	152
Anthraniloyl -O-glucose	H	322	138

C

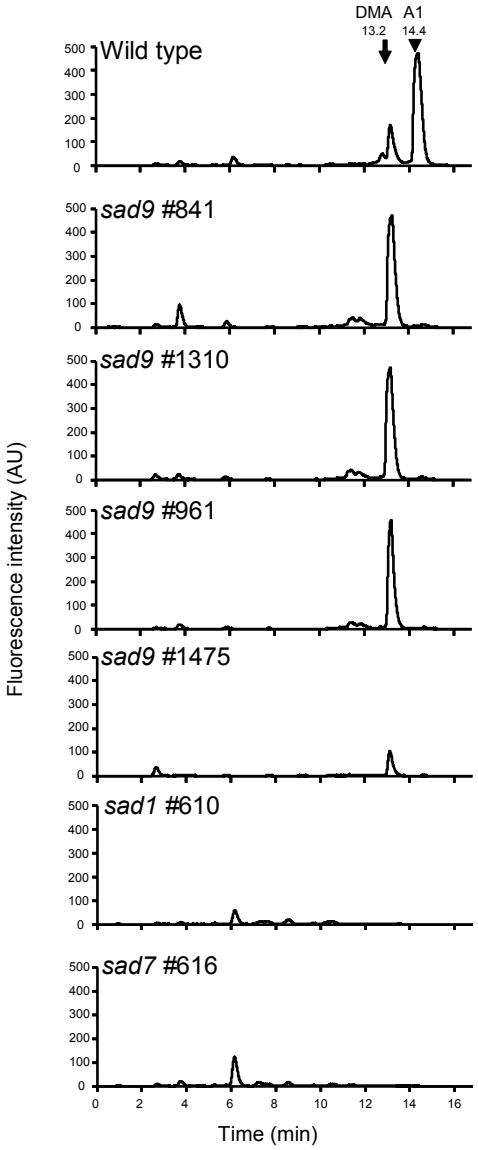

Supplemental Figure 2. Identification of des-methyl avenacin A-1 and anthraniloyl-*O*-glucose by LCMS.

(A) Mass spectra for avenacin A-1 (top, corresponding to the 14.4 min peak in the wild-type sample in Figure 4A), and des-methyl avenacin A-1 (bottom, corresponding to the 13.2 min peak in the *sad9* mutant #1310). Avenacin A-1 gives rise to major ions at *m/*z =1094 and 1116, the proton and sodium adducts. Corresponding ions 14 amu lighter (loss of CH_3) are seen in the *sad9* mutant at *m/*z =1080 and 1102. In-chamber fragmentation gives rise to the aglycone (AG) of avenacin A-1 at *m/z* = 638, and of des-methyl avenacin A-1 at 624, showing that the methyl group is missing from the aglycone and not the trisaccharide. The fluorescence emission maxima of the methanolic root extracts from wild type was found to be 440 nm compared to 410 nm from the *sad9* mutant. This is consistent with the fluorescence spectra of *N*-methyl anthranilate and anthranilate, respectively, and suggests that the methyl group is likely to be missing from the anthranilate acyl-group in the *sad9* mutants.

(B) Mass spectra for *N*-methyl anthraniloyl-*O*-glucose (NMA-glc; corresponding to the 6.2 min peak in the *sad7* mutant sample in Figure 4) and anthraniloyl-*O*-glucose (Anth-glc; corresponding to the 2.7 min peak in the *sad 9* mutant sample #1310 in Figure 4). NMA-glc gives rise to a major ion at *m/*z = 336 corresponding to the sodium adduct; and at 152, the proton adduct of the aglycone. Anth-glc produces corresponding ions 14 amu lighter than these at 322 and 138, indicating that a methyl group is missing from the aglycone.

(C) LC analysis with fluorescence detection of root-tip extracts shows the absence of avenacin A-1 (A1 indicated by the arrow head) and the presence of des-methyl avenacin A (DMA, indicated by arrow) in all *sad9* mutants. The *sad1* (#610) and *sad7* (#616) mutants lack both compounds.

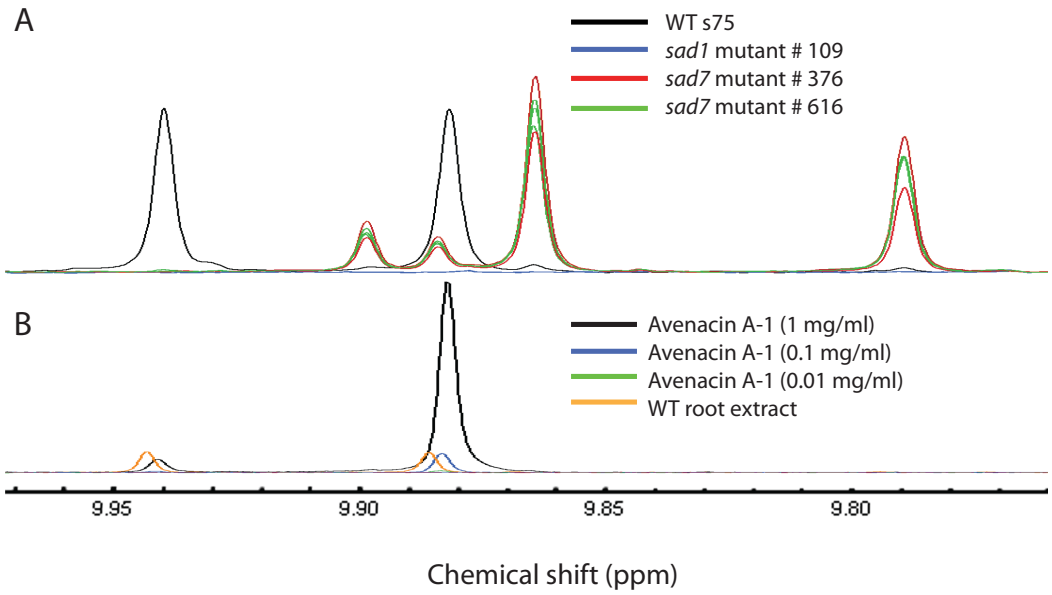

Supplemental Figure 3. ^{1}H-NMR spectra of the avenacin C30-aldehyde region in oat root extracts.

(A) Analysis of extracts of wild type (WT) and mutant oat roots. WT extracts show characteristic peaks at 9.88 and 9.94 ppm corresponding to the C-30 aldehyde of avenacins A-1 and A-2 respectively. The peaks present in the *sad7* mutants at 9.79 and 9.86 correspond to des-acyl avenacins. None of these peaks were detected in the avenacin-deficient *sad1* mutant. Spectra for several representative samples are shown for *sad7* mutants #616 and #376. (B) Avenacin A-1 standards with WT oat root extract for comparison. The avenacin A-1 standard has a low level of avenacin A-2 contamination. Oat roots were harvested from 2-week-old hydroponically grown plants, and were extracted in 70% deuterated methanol in D_2O (containing 51.6 µg/ml TSP as an internal standard), and spectra were collected using a 600MHz NMR spectrometer (Bruker). Total avenacin and des-acyl avenacin concentrations, pMols/mg fresh weight (± SEM, n=4): wild type, 6.11 ±0.41; *sad7* mutant #376: 8.54 ±1.08; *sad7*mutant #616: 7.16 ±0.89. Note that these values are based on extracts from whole root systems, in contrast to the values reported in the main text which are based on extracts from root tips.

Supplemental Figure 4

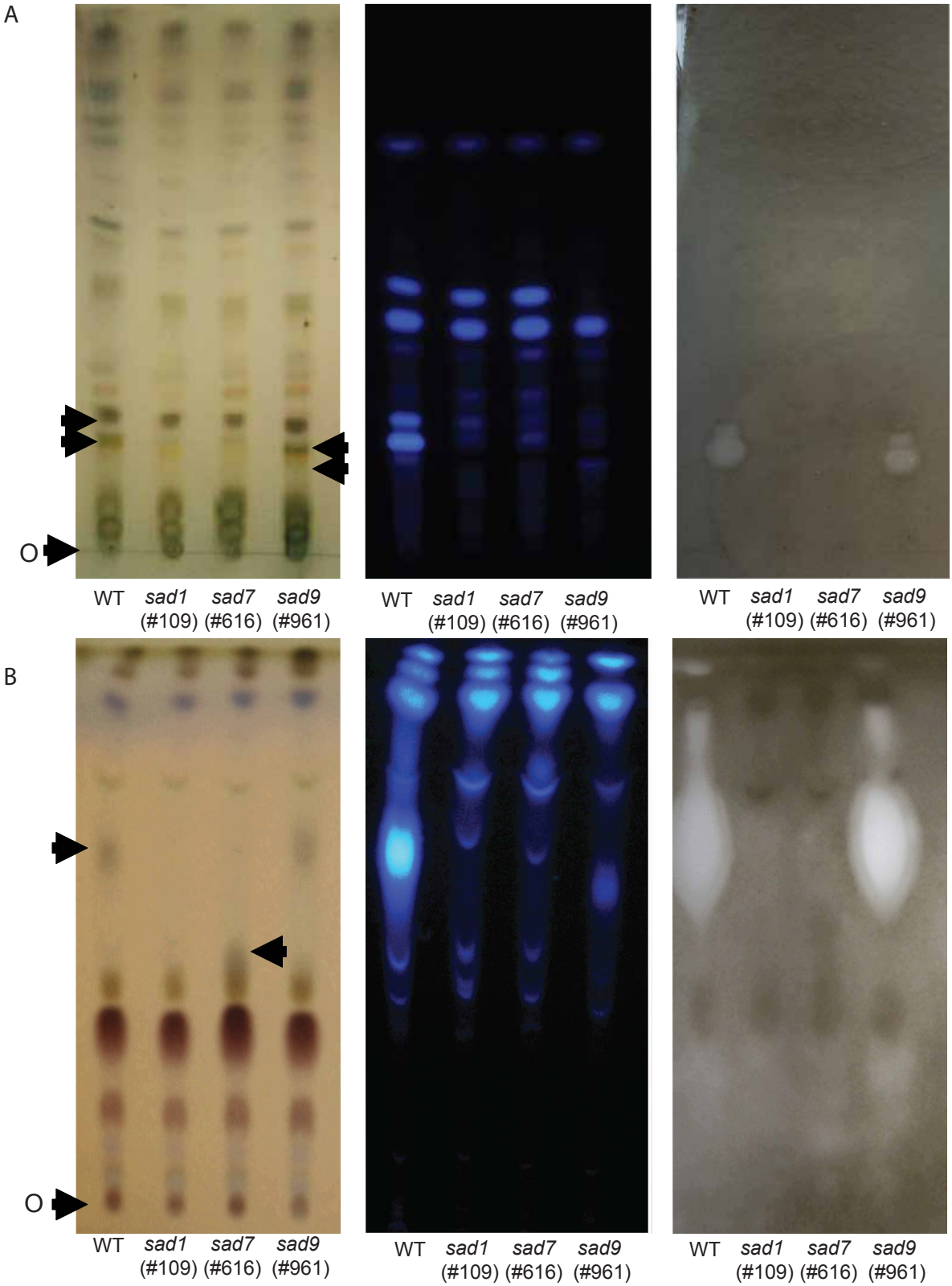

Supplemental Figure 4. Anti-fungal activity is associated the des-methyl avenacin A-1 in the *sad9* root extract, but not with des-acyl avenacin A in *sad7* root extract.

Extracts from equal weights of root tips from wild type or avenacin-deficient *sad1* (#109), *sad7* (#616), or *sad9* (#961) mutants were separated by thin layer chromatography, and visualised by *p*-anisaldehyde staining (left), UV-illumination (centre) or with a bioassay for the growth of *Colletotrichum orbiculare* (#NBRC 33130) (right). Samples were scraped from a replicate TLC plate in the areas indicated by arrows, and identified by mass spectrometry.

A: TLC was developed in chloroform:methanol:water at a ratio of 13:6:1. The two major fluorescent avenacins (A-1 and B-1) were detected in the WT samples indicated by the lower and upper arrows respectively, the non-fluorescent avenacin A-2 was also present at the same retention factor (Rf) as avenacin A-1. These are associated with two distinct zones of inhibition of *Colletotrichum* growth. These zones of inhibition are absent from *sad1* and *sad7* mutants that lack acylated avenacins, but present in the *sad9* mutant, where they are associated with the two detectable avenacins: des-methyl avenacin A (which has weak purple fluorescence) and avenacin A-2 (not fluorescent but associated with *p*-anisaldehyde stain (Avenacin B-2 is also present in *sad9* mutant roots, but at much lower levels (Supplemental Table 1)). This indicates that, as with other acylated avenacins, desmethyl avenacin A-1 possesses anti-fungal activity.

B: TLC was developed in chloroform:methanol:water at a ratio of 10:9:1. A similar zone of inhibition can be seen associated with the presence of acylated avenacins in the WT and *sad9* mutant (top arrow). The presence of desacyl avenacin A can be seen by *p*-anisaldehyde staining and no anti-fungal activity is associated with this compound, despite it's presence at similar levels to the acylated avenacins in the WT. O = origin. For staining; one replicate plate was sprayed with acetic acid:*p*-anisaldehyde:sulphuric acid (480:1:1), and heated at 130º C for 10 minutes. Growth assay for *Colletotrichum orbiculare* was performed as described in Tsurushima et al. (1995).

Supplemental Figure 5

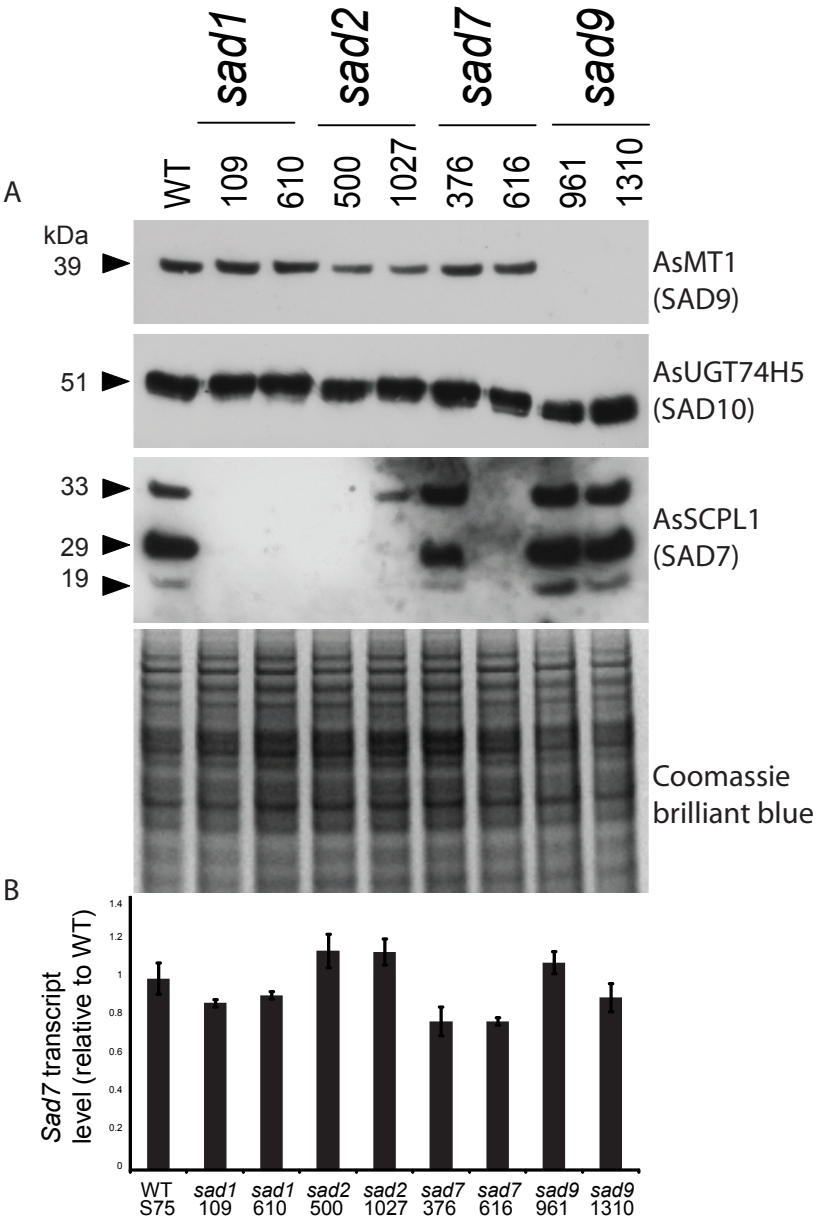

Supplemental Figure 5. As- SCPL1 expression is reduced or abolished in oat mutants blocked in the early steps in the synthesis of the avenacin triterpene.

(A) Immuno-blot analysis of soluble protein extracts from oat roots, probed with specific antisera raised against As- MT1, As- UGT74H5 and As- SCPL1. The bottom panel shows Coomassie brilliant blue-staining of a replicate gel. Protein extracts from root tips of 3-day-old seedlings were prepared from wild-type *Avena strigosa*, and *sad1* (#109 and #610), *sad2* (#500 and #1027), *sad7* (#376 and #616), and *sad9* (#961 and #1310) mutants. Bands corresponding to the predicted size of the MT1 and UGT74H5 proteins, and the predicted subunits of the mature SCPL1 protein (Mugford et al. 2009) were detected. (B) Analysis of *SCPL1* transcript levels in RNA extracted from 3-day-old root tips, measured by qPCR. RNA was extracted and cDNA synthesised as described previously (Qi et al. 2006). Expression values were normalised against the *Ef1a* transcript. Values are means (n=3, ±S.E.M). No significant differences were found between the wild type and any of the mutants ($p>0.05$, T-test with Bonferroni correction).

Supplemental Figure 6

A

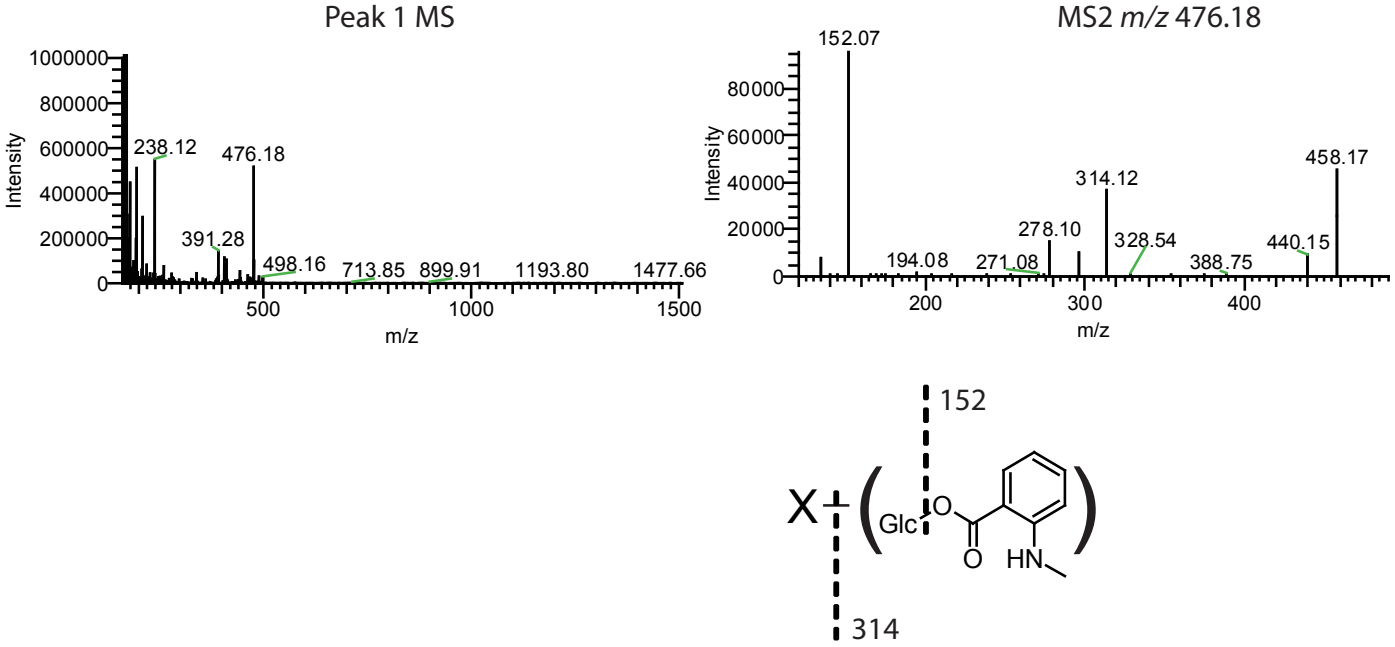

B

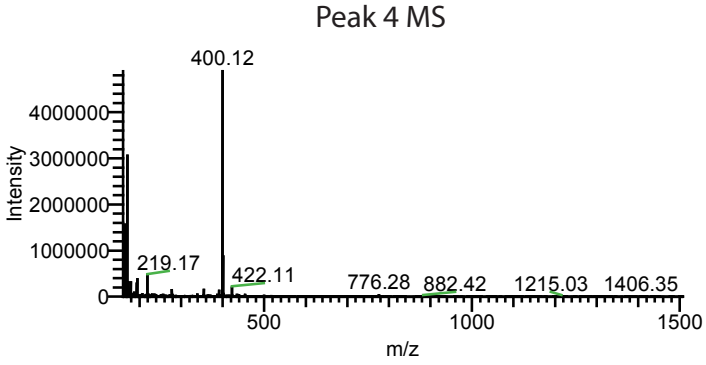

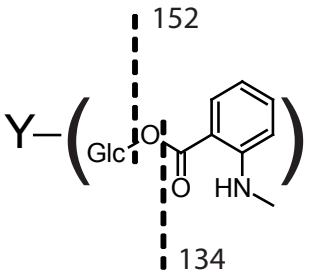

Supplemental Figure 6. LCMS analysis of fluorescent compounds from *N. benthamiana* plants co-expressing As- MT1 and As- UGT74H5.

Mass spectra (left) and MS2 fragmentation (right) of peak 1 (A) and peak 4 (B) from figure 4, together with a schematic showing the likely fragmentation events. The accurate mass of the compound in peak 1 = 476.1767 amu, which is consistent with $C_{20}H_{29}O_{12}N$ [M+H] (error = 0.84 ppm) or *N*-methyl anthraniloyl-*O*-glucose + a hexose (X). The mass of the compound in peak 4 is 400.1238, consistent with $C_{17}H_{21}O_{10}N$ [M+H] (error = 0.006 ppm) or *N*-methyl anthraniloyl-*O*-glucose + malate (Y).

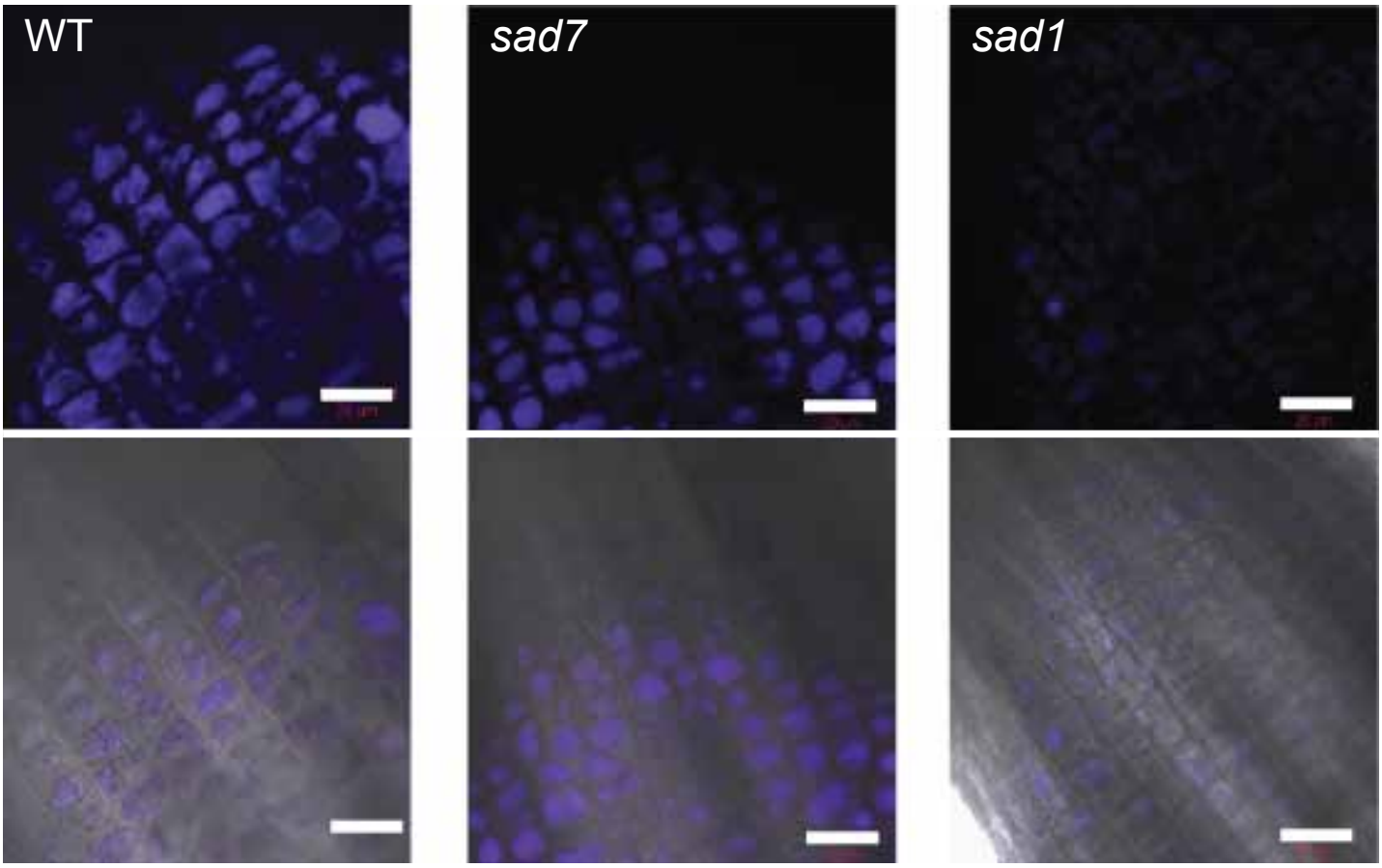

Supplemental Figure 7. **Fluorescent compounds accumulate in the vacuole of the *sad7* mutants.**

Optical sections of epidermal cells of root tips of 3-day-old seedlings of wild-type *A. strigosa* (WT), *sad7* mutant #616, and *sad1* mutant #610. Top, UV-fluorescence confocal microscopy; bottom, UV-fluorescence confocal microscopy overlayed with the bright field image. The same image acquisition and processing settings were used for the three images. Scale bars indicate 20 μm.

Supplemental Table 1. Quantification of avenacins and des-methyl avenacin A-1 in wild type and mutant oat root tips.

	Root tip avenacin concentrations (pMols per mg fresh weight)				
	Avenacin A-1	Avenacin B-1	Avenacin A-2	Avenacin B-2	Des-methyl avenacin A-1
WT	365.3 ±8.9	71.2 ±6.0	60.4 ±3.6	27.4 ±21.8	37.3 ±2.4
sad9 #961	n/d	n/d	65.0 ±17.5	13.6 ±2.5	109.0 ±29.9
sad9 #1310	n/d	n/d	114.5 ±7.8	13.6 ±1.3	189.2 ±26.5
sad1 #109	n/d	n/d	n/d	n/d	n/d
sad1 #610	n/d	n/d	n/d	n/d	n/d
sad7 #376	n/d	n/d	n/d	n/d	n/d
sad7 #616	n/d	n/d	n/d	n/d	n/d

Values are means (± SEM) of four biological replicates. Samples were analysed by high-pressure liquid chromatography (HPLC) coupled with mass spectrometry as described in Mugford et al. (2009). Avenacins A-1 and B-1 were quantified by fluorescence detection, and compared to a standard curve of N-methyl anthranilate; Des-methyl avenacin was quantified using a standard curve of anthranilate, and Avenacins A-2 and B-2 were quantified by UV-absorbance at 230 nm, and compared to a standard curve of benzoate. Values reported as n/d were below the detection limit, which was < 1 pMol/mg for all compounds.

Supplemental Table 2. Quantification of fluorescent compounds in *N. benthamiana* leaves co-expressing avenacin biosynthetic enzymes.

	Concentration in nmols of compound per mg leaf (dry weight) ± SEM							
Peak:	1		2		3		4	
Compound:	NMA-glc-glc		NMA-glc		NMA		NMA-glc-mal	
AsMT1 + UGT74H5 + SCPL1	8.52	±3.98	20.92	±4.85	3.52	±1.26	38.41	±14.16
AsMT1 + UGT74H5	13.00	±3.49	39.76	±6.46	7.34	±1.73	87.18	±18.04
AsMT1 +SCPL1	4.48	±2.67	4.73	±0.49	1.22	±0.63	11.61	±4.64
AsMT1	12.35	±5.77	11.93	±3.22	2.16	±0.97	20.02	±8.95
AsSCPL1	n/d		n/d		n/d		n/d	
UGT74H5	n/d		n/d		n/d		n/d	
UGT74H5+SCPL1	n/d		n/d		n/d		n/d	
EV	n/d		n/d		n/d		n/d	
P19	n/d		n/d		n/d		n/d	

Compounds were assayed for four replicate samples for each genotype by HPLC with fluorescence detection (Figure 4), and quantified using a standard curve of *N*-methyl anthranilate. NMA, *N*-methyl anthranilate; NMA-glc, *N*-methyl anthraniloyl-*O*-glucose; NMA-glc-glc and NMA-glc-mal, putative glucose- and malate- derivatives of *N*-methyl anthraniloyl-*O*-glucose, respectively. Values reported as n/d were below the detection limit, which was < 1 pMol/mg for all compounds.

Supplementary Table 3. Subcellular localisation of the AsMT1, AsUGT74H5 and AsSCPL1 proteins.

			Density (particles per μm^2)									
			Compartment									
Tissue	Genotype	Antisera	Cyt	Vac	Mit	Pla	ER	Wall	Nuc	Gol	Oth	Int
AsSCPL1 (SAD7)												
Oat root tip	WT	Anti-AsSCPL1	6.9 (21) ±0.5	**38.6 (20) ±4.2**	2.6 (16) ±0.8	6.1 (2)	5.8 (7) ±1.0	1.5 (9) ±0.6	2.0 (3) ±1.2	4.9 (2)	n/d	n/d
		PI	4.5 (12) ±0.7	1.8 (8) ±0.5	10.6 (12) ±2.4	n/d	3.7 (3) ±3.7	6.3 (8) ±1.7	6.2 (4) ±2.8	n/d	n/d	n/d
	sad7	Anti-AsSCPL1	2.2 (8) ±0.4	0.3 (14) ±0.2	2.0 (13) ±1.2	n/d	5.8 (3) ±3.4	0.0 (1)	3.6 (2) ±1.4	5.1 (2) ±5.1	n/d	n/d
AsMT1 (SAD9)												
Oat root tip	WT	Anti-AsMT1	**7.9 (12) ±0.7**	1.6 (11) ±0.4	4.7 (12) ±0.7	n/d	7.1 (5) ±2.2	3.0 (12) ±0.0	2.9 (5) ±1.5	5.9 (5) ±3.6	n/d	n/d
		PI	1.7 (8) ±0.2	5.0 (8) ±2.0	0.7 (12) ±0.7	n/d	2.2 (7) ±1.2	7.3 (6) ±2.5	1.3 (1)	1.5 (2)	n/d	n/d
	sad9	Anti-AsMT1	1.5 (7) ±0.4	2.3 (4) ±1.1	2.0 (6) ±0.8	n/d	3.6 (1)	0.3 (4) ±0.3	1.3 (1)	n/d	n/d	n/d
N. benthamiana leaf	*CPMV-AsMT1*	Anti-AsMT1	**29.1 (15) ±2.4**	2.6 (15) ±0.3	3.6 (13) ±0.8	6.6 (9) ±1.1	n/d	1.1 (15) ±0.5	6.9 (1)	n/d	0.0 (1)	2.5 (15) ±0.5
		PI	1.0 (8) ±0.1	1.0 (8) ±0.2	0.4 (5) ±0.2	0.7 (2) ±0.7	n/d	1.0 (8) ±0.5	n/d	n/d	n/d	0.7 (4) ±0.6
	CPMV-EV	Anti-AsMT1	1.5 (5) ±0.4	1.7 (5) ±0.1	7.4 (3) ±2.9	6.1 (1)	n/d	0.4 (3) ±0.4	n/d	n/d	n/d	0.5 (2)
AsUGT74H5 (SAD10)												
Oat root tip	WT	Anti-AsUGT74H5	**10.8 (12) ±0.4**	12.8 (11) ±1.0	3.1 (10) ±0.7	0.0 (1)	5.9 (1)	2.6 (10) ±1.2	8.5 (4) ±0.8	4.6 (3) ±4.6	n/d	n/d
		PI	1.7 (10) ±0.1	1.5 (9) ±0.4	1.4 (10) ±0.4	n/d	1.6 (8) ±0.5	2.0 (9) ±0.7	0.5 (2)	0.0 (1)	n/d	n/d
N. benthamiana leaf	*CPMV-UGT74H5*	Anti-AsUGT74H5	**74.8 (10) ±0.1**	2.8 (12) ±0.4	11.6 (10) ±3.5	6.3 (10) ±1.4	n/d	10.5 (6) ±6.0	n/d	n/d	n/d	1.5 (3) ±0.8
		PI	8.1 (8) ±1.2	2.4 (8) ±0.5	16.2 (4) ±3.0	13.0 (3) ±4.9	n/d	5.5 (8) ±2.8	n/d	n/d	0.0 (1)	n/d
	CPMV-EV	Anti-AsUGT74H5	2.0 (10) ±0.3	1.8 (8) ±0.5	3.5 (6) ±1.4	1.7 (6) ±0.7	n/d	1.2 (8) ±0.6	1.8 (2) ±1.8	n/d	0.0 (1)	n/d

Density (particles per μm^2) of gold particles in different subcellular compartments across replicate ultrathin tissue sections, from oat root tips or from *N. benthamiana* leaves, probed with anti-sera raised against the As- MT1, As- UGT74H5 or the As-SCPL1 proteins, or their corresponding pre-immune (PI) anti-sera. Values are mean particle densities measured across (n) replicate samples ± SEM. Values in bold indicate a compartment with significantly denser labelling in samples relative to the corresponding pre-immune sera experiment, and the corresponding mutant (where available) or empty vector control experiment ($p<0.05$, multiple linear regression). Cyt, cytoplasm; Vac, vacuole; Mit, mitochondira; Pla, plastid; ER, endoplasmic reticulum; Wall, cell wall; Nuc, nucleus; Gol, golgi; Oth, other; Int, intercellular space.

Supplemental References

Mugford, S.T., Qi, X., Bakht, S., Hill, L., Wegel, E., Hughes, R.K., Papadopoulou, K., Melton, R., Philo, M., Sainsbury, F., Lomonossoff, G.P., Deb Roy, A., Goss, R.J.M. and Osbourn, A. (2009). A serine carboxypeptidase-like acyltransferase is required for synthesis of antimicrobial compounds and disease resistance in oats. Plant Cell **21:** 2473-84.

Qi, X., Bakht, S., Qin, B., Leggett, M., Hemmings, A., Mellon, F., Eagles, J., Werck-Reichhart, D., Schaller, H., Lesot, A., Melton, R., and Osbourn, A. (2006). A different function for a member of an ancient and highly conserved cytochrome P450 family: from essential sterols to plant defense. Proc. Natl. Acad. Sci. USA **103:** 18848-18853.

Tsurushima, T., Ueno, T., Fukami, H., Irie, H., and Inoue, M. (1995) Germination self-inhibitors from *Colletotrichum gloeosporioides* f. sp. *Jussiaea*. MPMI **8**: 652-657.